Dual-Band Quasi-Elliptic Filter With Wide Upper Stopband in Hybrid SIW-Microstrip Technology

Yilong Zhu [#*1], Yuandan Dong [#2], Jens Bornemann [*3]

[#]*University of Electronic Science and Technology of China, Chengdu, Sichuan, China*
**Department of Electrical and Computer Engineering, University of Victoria, Victoria, BC, Canada*
[1]Yilong@std.uestc.edu.cn, [2]ydong@uestc.edu.cn, [3]j.bornemann@ieee.org

***Abstract* — A dual-band quasi-elliptic filter with wide stopband characteristics is presented. Two single-band cross-coupled filters, which are realized in hybrid microstrip and substrate integrated waveguide (SIW) technologies, are paralleled to construct the filter. To suppress SIW higher-order modes, orthogonal feeding ports are applied. In addition, due to the staggered resonant frequencies of the microstrip and SIW resonators, the next higher-order mode can be further degraded. To demonstrate the concept, a dual-band filter prototype centered at 8 GHz and 10.5 GHz is designed, fabricated and measured. Its experimental results show good agreement with simulations, exhibiting high selectivity and wide-stopband characteristics.**

Index Terms — Dual-band filter, hybrid microstrip and SIW, high selectivity, quasi-elliptic response, wide stopband.

I. INTRODUCTION

Substrate integrated waveguide (SIW) dual-band filters have drawn significant attention to meet increasing requirements of multi-standard services and multi-channel communications. However, compared to microstrip filters, SIW filters suffer from the unneglectable issue of spurious bands. To solve this problem, numerous techniques have been proposed, including employing low-pass filters at feeding ports [1], constructing coupling-null structures [2], using orthogonal feeding ports [3], and cascading dissimilar resonators [4], [5]. All these works are able to achieve single-band wide-stopband responses, but dual-band filters with wide upper stopbands are rarely studied. Recently, it has become popular to design dual-band filters by using SIW dual-mode resonances [6-8]. For example, dual-band filters utilizing the TE_{201} mode to create the second passbands are reported in [6], [7]; by using TE_{301} and TE_{102} modes, an extended frequency ratio can be achieved in [8]. However, wide-stopband characteristics are not discussed for these filters.

Therefore, in this paper, by combining microstrip and SIW technologies, a dual-band quasi-elliptic filter with wide upper stopband is presented. Two single-band filters, which are constructed by hybrid microstrip and SIW resonators, are combined to achieve the proposed dual-band design. The microstrip resonators not only resonate to generate transmission poles (TPs), but also introduce cross couplings to create transmission zeros (TZs), resulting in improved selectivity. To achieve wide-stopband performance, orthogonal feeding ports are applied to suppress higher-order SIW modes. In addition, these modes can be further suppressed due to the staggered resonant frequencies of the microstrip and SIW resonators.

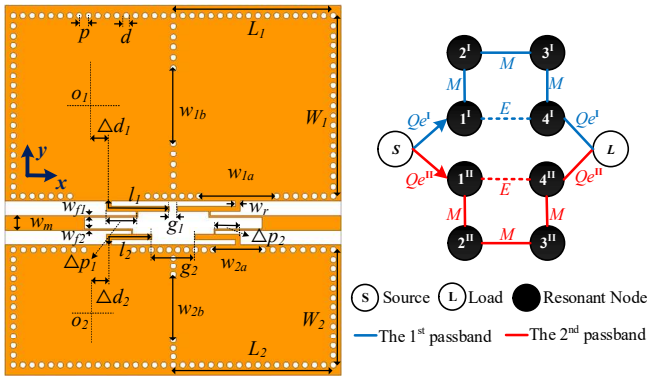

(a) (b)

Fig. 1. (a) Layout of the proposed dual-band quasi-elliptic filter with wide stopband. (b) Its coupling schematic topology. (Initial dimensions in mm: L_1= L_2=16.05, W_1=17.8, W_2=11.6, w_{1a}=7.8, w_{2a}=5, w_{1b}=7.6, w_{2b}=6.6, $\triangle d_1$ =$\triangle d_2$ = 1.55, l_1 = 6.85, l_2 = 5.07, g_1 = 0.75, g_2 = 4.31, $\triangle p_1$ = 3.08, $\triangle p_2$ = 2.57, w_r = 0.5, w_{f1} = 0.17, w_{f2} = 0.14, w_m = 1.57, p< 1, d = 0.6.)

II. DUAL-BAND FILTER DESIGN AND ANALYSIS

A. Configuration and Coupling Topology

Fig. 1(a) shows the proposed dual-band filter, which is realized by paralleling two single-band filters. Each single-band filter is composed by a pair of quarter-wavelength microstrip resonators and two rectangular SIW cavities. Grounded coplanar-waveguide (GCPW) feeding lines, which are placed between the SIW cavities, are used to excite the microstrip resonators. By arranging the open ends close to each other, an electric coupling can be realized between each pair of the quarter-wavelength resonators, which is considered as cross couplings. Additionally, other couplings, such as the couplings between the microstrip and SIW resonators, and the couplings between two SIW cavities, are realized by the inductive coupling windows w_{1a}, w_{1b}, w_{2a}, w_{2b} (Fig. 1(a)), which are considered as magnetic couplings.

Based on such a filter configuration, its coupling schematic topology can be drawn as shown in Fig. 1(b), where the superscripts I and II denote the first and second passband, respectively. All couplings on the main transmission path are magnetic, while they are electric on the cross-coupling transmission paths.

B. Synthesis and Design

For quarter-wavelength resonators and SIW cavities, their resonant frequencies can be calculated by

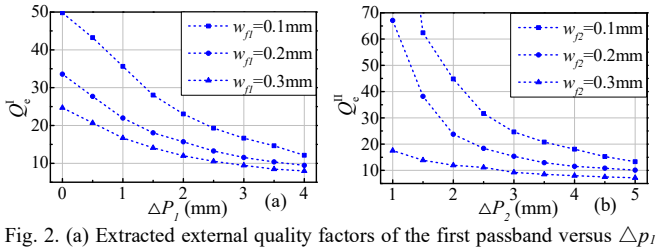

Fig. 2. (a) Extracted external quality factors of the first passband versus $\triangle p_1$ with w_{f1} as a variable. (b) Extracted external quality factors of the second passband versus $\triangle p_2$ with w_{f2} as a variable.

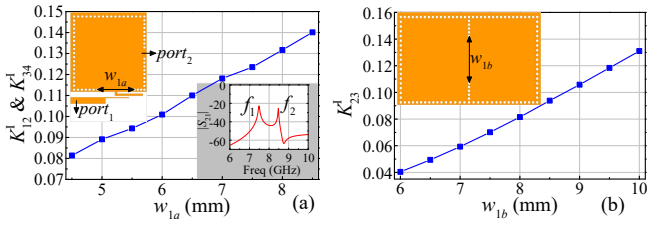

Fig. 3. (a) Extracted design curves of K_{12}^I (or K_{34}^I) versus w_{1a}. (b) Extracted design curves of K_{23}^I versus w_{1b}.

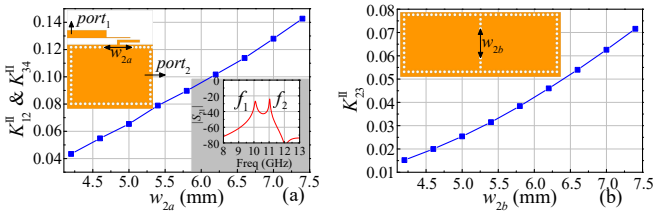

Fig. 4. (a) Extracted design curves of K_{12}^{II} (or K_{34}^{II}) versus w_{2a}. (b) Extracted design curves of K_{23}^{II} versus w_{2b}.

$$f_i = \frac{c}{\sqrt{\varepsilon_e}} \frac{\pi}{2l_i} \tag{1}$$

$$f_{TE_{m0n}} = \frac{c}{2\sqrt{\mu_r \varepsilon_r}} \sqrt{\left(\frac{m}{L_i}\right)^2 + \left(\frac{n}{W_i}\right)^2} \tag{2}$$

where c is the speed of light in vacuum, and ε_e is the equivalent relative permittivity for the microstrip resonators. L_i and W_i are the equivalent lengths and widths of the SIW cavities, while m and n are the mode indices along width and length directions, respectively; ε_r and μ_r represent the relative permittivity and permeability of the substrate (i =1, 2).

Initial dimensions of the resonators can be obtained once the two central frequencies of the filter are determined. To prototype the proposed concept, the dual-band filter is synthesized with a 4th-order quasi-elliptic response, whose central frequencies are located at 8 GHz and 10.5 GHz with a return loss of 20 dB for both passbands. The equal-ripple bandwidths are 760 MHz (Δ_1= 9.5%) for the first passband, and 810 MHz (Δ_2= 7.7%) for the second passband. The finite TZs are placed at Ω_1 = ±2.18 and Ω_2 = ±2.85, respectively. Using coupling matrix methods, the synthesized parameters can be calculated as follows

$$K_{12}^{\mathrm{I}} = K_{34}^{\mathrm{I}} = 0.086, K_{23}^{\mathrm{I}} = 0.073,$$
$$K_{14}^{\mathrm{I}} = -0.0105, Q_e^{\mathrm{I}} = 9.83,$$
$$K_{12}^{\mathrm{II}} = K_{34}^{\mathrm{II}} = 0.069, K_{23}^{\mathrm{II}} = 0.056,$$
$$K_{14}^{\mathrm{II}} = -0.0054, Q_e^{\mathrm{II}} = 12.5,$$

where Q_e and K_{ij} represent the external quality factors and coupling coefficients, respectively.

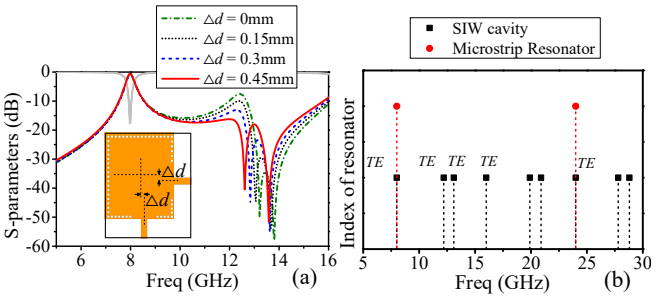

Fig. 5. (a) Simulated S-parameters of the SIW cavity versus increasing offset of the feeding ports. (b) Theoretical resonant frequencies of the SIW cavities and the quarter-wavelength resonators.

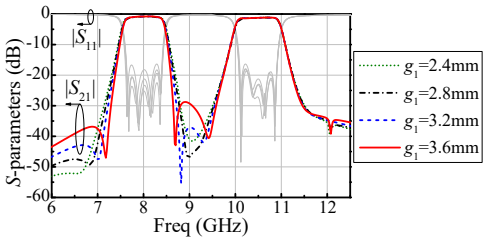

Fig. 6. Simulated S-parameters versus the gap g_1 of the first pair of quarter-wavelength resonators.

To clarify the design procedure, the extracted external quality factors for the two passbands are presented in Fig.2, which decrease with the increased offset of excitation positions at the microstrip resonators ($\triangle p_1$ and $\triangle p_2$). The widths of the feeding ports (w_{f1} and w_{f2}) show a significant impact as well, and wider feeding ports lead to lower external quality factors, namely larger coupling strength. As for coupling coefficients between the resonators, they can be controlled by adjusting widths w_{1a}, w_{1b}, w_{2a}, w_{2b} of the inductive coupling windows as shown in Figs. 3(a), 3(b), 4(a) and 4(b). Generally, the wider windows would lead to larger couplings. As for cross couplings between each pair of microstrip resonators, they can be produced by adjusting their gaps g_1 and g_2.

C. Suppression of Higher-Order Modes

As described in [3], orthogonal feeding ports are able to suppress SIW spurious bands, which can disable resonant effects of the TE_{201} and TE_{102} modes. Fig. 5(a) shows the simulated S-parameters of a SIW cavity, whose spurious bands are gradually suppressed with increasing offset of the feeding ports. Note that in this process, there is little impact on the passband. Furthermore, staggered resonant frequencies of the microstrip and SIW resonators contribute to suppression of the spurious bands. As shown in Fig. 5(b), the microstrip and SIW resonators have the same fundamental resonant frequencies but staggered higher-order frequencies, except for the frequency where the TE_{303} mode overlaps with the first higher-order mode of the microstrip resonator. Therefore, higher-order SIW modes can be suppressed to a certain extent because they are unable to completely resonate in the microstrip resonators.

D. Controllable Transmission Zeros

Since the cross couplings are realized by the open ends of each pair of the microstrip resonators, they can be controlled by

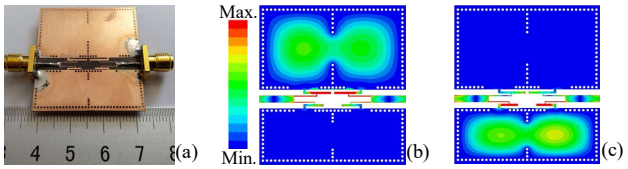

Fig. 7. (a) Photograph of the fabricated filter. (b) Electric field distributions of the 1st passband at 8 GHz, and (c) the 2nd passband at 11.5 GHz.

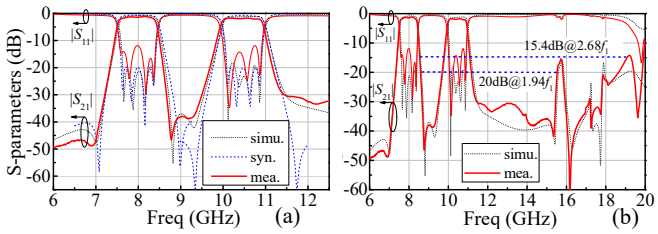

Fig. 8. (a) Simulated, measured and synthesized *S*-parameters covering a narrow frequency band of 6-12.5 GHz. (b) Simulated and measured *S*-parameters covering a wide frequency band of 6-20 GHz.

tuning the gaps. As shown in Fig. 6, two TZs appear on both sides of each passband when slightly decreasing the gap (g_1), resulting in improved selectivity with little impact on the passband performance. This is also applicable for the second passband by tuning the other gap (g_2).

III. FABRICATION, MEASUREMENT, AND DISCUSSION

The filter fabrication is based on 508 μm Rogers RT/duroid 5880 substrate (ε_r = 2.2, tanδ = 0.0009). Fig. 7(a) shows a photograph of the manufactured filter, whose overall circuit size is 37.07mm×33.7 mm (1.61λ_g×1.46λ_g). Figs. 7(b) and 7(c) depict the electric field distributions of the two passbands, in which two transmission paths are created independently by the upper and lower resonators, respectively.

Fig. 8(a) presents the simulated, measured and synthesized *S*-parameters, which are in agreement. For both passbands, the measured in-band return losses are better than 11.8 dB. The measured center frequencies are located at 7.97 GHz for the 1st passband and 10.44 GHz for the 2nd passband, exhibiting minor offsets compared to the simulated of 8 GHz and 10.5 GHz. The measured insertion losses (ILs) including those of SMA connectors are 1.15 dB and 1.7 dB, respectively, while the simulated ILs are 0.78 dB and 1.17 dB. The measured 3-dB bandwidths of the two passbands are 919 MHz (Δ_1= 11.5%) and 1014 MHz (Δ_2= 9.7%) compared to simulations of 910 MHz (Δ_1= 11.4%) and 1000 MHz (Δ_2= 9.5%). As expected, the proposed filter shows high selectivity with TZs created at both sides of each passband. Fig. 8(b) shows the simulated and measured *S*-parameters covering a wider frequency range (5-20 GHz). As expected, the proposed dual-band filter presents a wide-stopband response with a rejection level of 20 dB up to 1.94 f_1 (or 15.4 dB up to 2.68 f_1), where f_1 is the center frequency of the first passband.

A comparison with other reported works is presented in Table I. The proposed filter shows wider bandwidths and lower insertion losses for both passbands, and the wide stopband characteristic is an added benefit. Additionally, since electric couplings are realized by the microstrip resonators, an extra negative coupling structure (NCS), which is used in [6] and [8], is not necessary in this filter configuration.

TABLE I
COMPARISON OF STATE-OF-ART FILTERS

Ref.	[6]-III	[7]	[8]-II	This work
Technology	SIW	SIW & microstrip	HMSIW	SIW & microstrip
Order	4/4	4/4	4/4	4/4
f_1/f_2 (GHz)	12/17	8.05/9.99	5/8.5	8/10.5
$k = f_2/f_1$	1.42	1.24	1.7	1.31
3-dB FBW (%)	5.08/2.72	9.1/6.2	6.26/7.75	11.5/9.7
IL (dB)	1.39/2.47	1.74/2.21	2.02/1.82	1.15/1.7
An extra NCS	Y	N	Y	N
No. of TZs	5	4	4	4
Control of TZs	Y	Y	Y	Y
size($\lambda_g \times \lambda_g$)	2.11×1.37	1.13×1.02	0.84×1.31	1.61×1.46
Stopband Rejection	>20 dB up to 1.56f_1	>20 dB up to 1.53f_1	>20 dB up to 1.96f_1 >10 dB up to 2.04f_1	>20 dB up to 1.94f_1 >15.4 dB up to 2.68f_1

NCS: negative coupling structure

IV. CONCLUSION

A dual-band quasi-elliptic filter realized by hybrid microstrip and SIW resonators is presented, which shows excellent performance of wide stopband response and high selectivity. Coupling-matrix-based design procedures are described, and suppression of SIW higher-order modes are illustrated. The suppression, which is mainly achieved by orthogonal feeding ports, can be further improved by staggered resonant frequencies of the microstrip and SIW resonators.

REFERENCES

[1] S. Y. Zheng, Z. L. Su, Y. M. Pan, Z. Qamar, and D. Ho, "New dual-/tri-band bandpass filters and diplexer with large frequency ratio," *IEEE Trans. Microw. Theory Techn.*, vol. 66, no. 6, pp. 2978-2992, June 2018.

[2] A. R. Azad and A. Mohan, "Substrate integrated waveguide dual-band and wide-stopband bandpass filters," *IEEE Microw. Wireless Compon. Lett.*, vol. 28, no. 8, pp. 660-662, Aug. 2018.

[3] P. Chu, L. Guo, L. Zhang, F. Xu, W. Hong, and K. Wu, "Wide stopband substrate integrated waveguide filter implemented by orthogonal ports' offset," *IEEE Trans. Microw. Theory Techn.*, vol. 68, no. 3, pp. 964-970, March 2020.

[4] M. Salehi and E. Mehrshahi, "Spurious-response suppression of substrate integrated waveguide filters using multishape resonators and slotted plane structures," *Int. J. RF Microw. Comput.-Aided Eng.*, vol. 21, no. 6, pp. 650–657, Nov. 2011.

[5] Y. Zhu and Y. Dong, "A novel compact wide-stopband filter with hybrid structure by combining SIW and microstrip technologies," *IEEE Microw. Wireless Compon. Lett.*, vol. 31, no. 7, pp. 841-844, July 2021.

[6] K. Zhou, C. Zhou, and W. Wu, "Resonance characteristics of substrate-integrated rectangular cavity and their applications to dual-band and wide-stopband bandpass filters design," *IEEE Trans. Microw. Theory Techn.*, vol. 65, no. 5, pp. 1511-1524, May 2017.

[7] Y. Zhu and Y. Dong, "A compact dual-band quasi-elliptic filter based on hybrid SIW and microstrip technologies," *IEEE Trans. Circuits Syst. II, Exp. Briefs*, vol. 69, no. 3, pp. 719-723, March 2022.

[8] K. Zhou, C. Zhou, and W. Wu, "Dual-mode characteristics of half-mode SIW rectangular cavity and applications to dual-band filters with widely separated passbands," *IEEE Trans. Microw. Theory Techn.*, vol. 66, no. 11, pp. 4820-4829, Nov. 2018.